

Learning Retrospective Knowledge with Reverse Reinforcement Learning

Shangtong Zhang^{*}
University of Oxford

Vivek Veeriah
University of Michigan, Ann Arbor

Shimon Whiteson
University of Oxford

Abstract

We present a Reverse Reinforcement Learning (Reverse RL) approach for representing *retrospective knowledge*. General Value Functions (GVFs) have enjoyed great success in representing *predictive knowledge*, i.e., answering questions about possible future outcomes such as “how much fuel will be consumed in expectation if we drive from A to B?”. GVFs, however, cannot answer questions like “how much fuel do we expect a car to have given it is at B at time t ?”. To answer this question, we need to know when that car had a full tank and how that car came to B. Since such questions emphasize the influence of possible past events on the present, we refer to their answers as *retrospective knowledge*. In this paper, we show how to represent retrospective knowledge with Reverse GVFs, which are trained via Reverse RL. We demonstrate empirically the utility of Reverse GVFs in both representation learning and anomaly detection.

1 Introduction

Much knowledge can be represented by answers to predictive questions (Sutton, 2009), for example, “to know that Joe is in the coffee room is to predict that you will see him if you went there” (Sutton, 2009). Such knowledge is referred to as *predictive knowledge* (Sutton, 2009; Sutton et al., 2011). General Value Functions (GVFs, Sutton et al. 2011) are commonly used to represent predictive knowledge. GVFs are essentially the same as canonical value functions (Puterman, 2014; Sutton and Barto, 2018). However, the policy, the reward function, and the discount function associated with GVFs are usually carefully designed such that the numerical value of a GVF at certain states matches the numerical answer to certain predictive questions. In this way, GVFs can represent predictive knowledge.

Consider the concrete example in Figure 1, where a microdrone is doing a random walk. The microdrone is initialized somewhere with 100% battery. L4 is a power station where its battery is recharged to 100%. Each clockwise movement consumes 2% of the battery, and each counterclockwise movement consumes 1% (for simplicity, we assume negative battery levels, e.g., -10%, are legal). Furthermore, each movement fails with probability 1%, in which case the microdrone remains in the same location and no energy is consumed. An example of a predictive question in this system is:

Question 1. *Starting from L1, how much energy will be consumed in expectation before the next charge?*

To answer this question, we can model the system as a Markov Decision Process (MDP). The policy is uniformly random and the reward for each movement is the

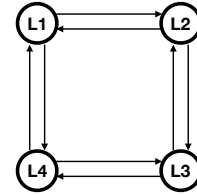


Figure 1: A microdrone doing random walk among four different locations. L4 is a charging station where the microdrone’s battery is fully recharged.

^{*}Correspondence to shangtong.zhang@cs.ox.ac.uk

additive inverse of the corresponding battery consumption. Whenever the microdrone reaches state L4, the episode terminates. Under this setup, the answer to Question 1 is the expected cumulative reward when starting from L1, i.e., the state value of L1. Hence, GVFs can represent the predictive knowledge in Question 1. As a GVF is essentially a value function, it can be trained with any data stream from agent-environment interaction via Reinforcement Learning (RL, Sutton and Barto 2018), demonstrating the generality of the GVF approach. However, the most appealing feature of GVFs is their compatibility with off-policy learning, making this representation of predictive knowledge scalable and efficient. For example, in the Horde architecture (Sutton et al., 2011), many GVFs are learned in parallel with gradient-based off-policy temporal difference methods (Sutton et al., 2009b,a; Maei, 2011). In the microdrone example, we can learn the answer to Question 1 under many different conditions (e.g., when the charging station is located at L2 or when the microdrone moves clockwise with probability 80%) simultaneously with off-policy learning by considering different reward functions, discount functions, and policies.

GVFs, however, cannot answer many other useful questions, e.g., if at some time t , we find the microdrone at L1, how much battery do we expect it to have? As such questions emphasize the influence of possible past events on the present, we refer to their answers as *retrospective knowledge*. Such retrospective knowledge is useful, for example, in anomaly detection. Suppose the microdrone runs for several weeks by itself while we are traveling. When we return at time t , we find the microdrone is at L1. We can then examine the battery level and see if it is similar to the expected battery at L1. If there is a large difference, it is likely that there is something wrong with the microdrone. There are, of course, many methods to perform such anomaly detection. For example, we could store the full running log of the microdrone during our travel and examine it when we are back. The memory requirement to store the full log, however, increases according to the length of our travel. By contrast, if we have retrospective knowledge, i.e., the expected battery level at each location, we can program the microdrone to log its battery level at each step (overwriting the record from the previous step). We can then examine the battery level when we are back and see if it matches our expectation. The current battery level can be easily computed via the previous battery level and the energy consumed at the last step, using only constant computation per step. The storage of the battery level requires only constant memory as we do not need to store the full history, which would not be feasible for a microdrone. Thus retrospective knowledge provides a memory-efficient way to perform anomaly detection. Of course, this approach may have lower accuracy than storing the full running log. This is indeed a trade-off between accuracy and memory, and we expect applications of this approach in memory-constrained scenarios such as embedded systems.

To know the expected battery level at L1 at time t is essentially to answer the following question:

Question 2. *How much energy do we expect the microdrone to have consumed since the last time it had 100% battery given that it is at L1 at time t ?*

Unfortunately, GVFs cannot represent retrospective knowledge (e.g., the answer to Question 2) easily. GVFs provide a mechanism to ignore all future events after reaching certain states via setting the discount function at those states to be 0. This mechanism is useful for representing predictive knowledge. For example, in Question 1, we do not care about events *after* the next charge. For retrospective knowledge, we, however, need a mechanism to ignore all previous events before reaching certain states. For example, in Question 2, we do not care about events *before* the last time the microdrone had 100% battery. Unfortunately, GVFs do not have such a mechanism. In Appendix A, we describe several tricks that attempt to represent retrospective knowledge with GVFs and explain why they are invalid.

In this paper, we propose *Reverse GVFs* to represent retrospective knowledge. Using the same MDP formulation of the microdrone system, let the random variable \bar{G}_t denote the energy the microdrone has consumed at time t since the last time it had 100% battery. To answer Question 2, we are interested in the conditional expectation of \bar{G}_t given that $S_t = \text{L1}$. We refer to such conditional expectations as Reverse GVFs, which we propose to learn via *Reverse Reinforcement Learning*. The key idea of Reverse RL is still bootstrapping, but in the reverse direction. It is easy to see that \bar{G}_t depends on \bar{G}_{t-1} and the energy consumption from $t-1$ to t . In general, in Reverse RL, the quantity of interest at time t depends on that at time $t-1$. This idea of bootstrapping from the past has been explored by Wang et al. (2007, 2008); Hallak and Mannor (2017); Gelada and Bellemare (2019); Zhang et al. (2020c) but was limited to the density ratio learning setting. We propose several Reverse RL algorithms and prove their convergence under linear function approximation. We also propose Distributional Reverse RL algorithms akin to Distributional RL (Bellemare et al., 2017; Dabney

et al., 2017; Rowland et al., 2018) to compute the probability of an event for anomaly detection. We demonstrate empirically the utility of Reverse GVFs in anomaly detection and representation learning.

Besides Reverse RL, there are other approaches we could consider for answering Question 2. For example, we could formalize it as a simple regression task, where the input is the location and the target is the power consumption since the last time the microdrone had 100% battery. We show below that this regression formulation is a special case of Reverse RL, similar to how Monte Carlo is a special case of temporal difference learning (Sutton, 1988). Alternatively, answering Question 2 is trivial if we have formulated the system as a Partially Observable MDP. We could use either the location or the battery level as the state and the other as the observation. In either case, however, deriving the conditional observation probabilities is nontrivial. We could also model the system as a reversed chain directly as Morimura et al. (2010) in light of reverse bootstrapping. This, however, creates difficulties in off-policy learning, which we discuss in Section 5.

2 Background

We consider an infinite-horizon Markov Decision Process (MDP) with a finite state space \mathcal{S} , a finite action space \mathcal{A} , a transition kernel $p : \mathcal{S} \times \mathcal{S} \times \mathcal{A} \rightarrow [0, 1]$, and an initial distribution $\mu_0 : \mathcal{S} \rightarrow [0, 1]$. In the GVF framework, users define a reward function $r : \mathcal{S} \times \mathcal{A} \rightarrow \mathbb{R}$, a discount function $\gamma : \mathcal{S} \rightarrow [0, 1]$, and a policy $\pi : \mathcal{A} \times \mathcal{S} \rightarrow [0, 1]$ to represent certain predictive questions. An agent is initialized at S_0 according to μ_0 . At time step t , the agent at state S_t selects an action A_t according to $\pi(\cdot|S_t)$, receives a bounded reward R_{t+1} satisfying $\mathbb{E}[R_{t+1}] = r(S_t, A_t)$, and proceeds to the next state S_{t+1} according to $p(\cdot|S_t, A_t)$. We then define the return at time step t recursively as

$$G_t \doteq R_{t+1} + \gamma(S_{t+1})G_{t+1},$$

which allows us to define the general value function $v_\pi(s) \doteq \mathbb{E}[G_t|S_t = s]$.² The general value function v_π is essentially the same as the canonical value function (Puterman, 2014; Sutton and Barto, 2018). The name general emphasizes its usage in representing predictive knowledge. In the microdrone example (Figure 1), we define the reward function as $r(s, a_1) = 2, r(s, a_2) = 1 \forall s$, where a_1 is moving clockwise and a_2 is moving counterclockwise. We define the discount function as $\gamma(L1) = \gamma(L2) = \gamma(L3) = 1, \gamma(L4) = 0$. Then it is easy to see that the numerical value of $v_\pi(L1)$ is the answer to Question 1. In the rest of the paper, we use functions and vectors interchangeably, e.g., we also interpret v_π as a vector in $\mathbb{R}^{|\mathcal{S}|}$. Furthermore, all vectors are column vectors.

The general value function v_π is the unique fixed point of the generalized Bellman operator \mathcal{T} (Yu et al., 2018): $\mathcal{T}y \doteq r_\pi + P_\pi \Gamma y$, where $P_\pi \in \mathbb{R}^{|\mathcal{S}| \times |\mathcal{S}|}$ is the state transition matrix, i.e., $P_\pi(s, s') \doteq \sum_a \pi(a|s) p(s'|s, a)$, $r_\pi \in \mathbb{R}^{|\mathcal{S}|}$ is the reward vector, i.e., $r_\pi(s) \doteq \sum_a \pi(a|s) r(s, a)$, and $\Gamma \in \mathbb{R}^{|\mathcal{S}| \times |\mathcal{S}|}$ is a diagonal matrix whose s -th diagonal entry is $\gamma(s)$. To ensure v_π is well-defined, we assume π and γ are defined such that $(I - P_\pi \Gamma)^{-1}$ exists (Yu, 2015). Then if we interpret $1 - \gamma(s)$ as the probability for an episode to terminate at s , we can assume termination occurs w.p. 1.

3 Reverse General Value Function

Inspired by the return G_t , we define the reverse return \bar{G}_t , which accumulates previous rewards:

$$\bar{G}_t \doteq R_t + \gamma(S_{t-1})\bar{G}_{t-1}, \quad \bar{G}_0 \doteq 0.$$

In the reverse return \bar{G}_t , the discount function γ has different semantics than in the return G_t . Namely, in G_t , the discount function down-weights future rewards, while in \bar{G}_t , the discount function down-weights past rewards. In an extreme case, setting $\gamma(S_{t-1}) = 0$ allows us to ignore all the rewards before time t when computing the reverse return \bar{G}_t , which is exactly the mechanism we need to represent retrospective knowledge.

Let us consider the microdrone example again (Figure 1) and try to answer Question 2. Assume the microdrone was initialized at L3 at $t = 0$ and visited L4 and L1 afterwards. Then it is easy to

²For a full treatment of GVFs, one can use a transition-dependent reward function $r : \mathcal{S} \times \mathcal{S} \times \mathcal{A} \rightarrow \mathbb{R}$ and a transition-dependent discount function $\gamma : \mathcal{S} \times \mathcal{S} \times \mathcal{A} \rightarrow [0, 1]$ as suggested by White (2017). In this paper, we consider $r : \mathcal{S} \times \mathcal{A} \rightarrow \mathbb{R}$ and $\gamma : \mathcal{S} \rightarrow [0, 1]$ for the ease of presentation. All the results presented in this paper can be directly extended to transition-dependent reward and discount functions.

see that \bar{G}_2 is exactly the energy the microdrone has consumed since its last charge. In general, if we find the microdrone at L1 at time t , the expectation of the energy that the microdrone has consumed since its last charge is exactly $\mathbb{E}_{\pi,p,r}[\bar{G}_t|S_t = \text{L1}]$. Note the answer to Question 2 is not homogeneous in t . For example, suppose the microdrone is initialized at L4 at $t = 0$. If we find it at L1 at $t = 1$, it is trivial to see the microdrone has consumed 2% battery. By contrast, if we find it at L1 at $t = 100$, computing the energy consumption since the last time it had 100% battery is nontrivial. It is inconvenient that the answer depends the time step t but fortunately, we can show the following:

Assumption 1. *The chain induced by π is ergodic and $(I - P_\pi^\top \Gamma)^{-1}$ exists.*

Theorem 1. *Under Assumption 1, the limit $\lim_{t \rightarrow \infty} \mathbb{E}[\bar{G}_t|S_t = s]$ exists, which we refer to as $\bar{v}_\pi(s)$. Furthermore, we define the reverse Bellman operator \bar{T} as*

$$\bar{T}y \doteq D_\pi^{-1} \tilde{P}_\pi^\top \tilde{D}_\pi r + D_\pi^{-1} P_\pi^\top \Gamma D_\pi y,$$

where $D_\pi \doteq \text{diag}(d_\pi) \in \mathbb{R}^{|\mathcal{S}| \times |\mathcal{S}|}$ with d_π being the stationary distribution of the chain induced by π , $\tilde{P}_\pi \in \mathbb{R}^{|\mathcal{S}| \times |\mathcal{A}| \times |\mathcal{S}|}$ is the transition matrix, i.e., $\tilde{P}_\pi((s, a), s') \doteq p(s'|s, a)$, and $\tilde{D}_\pi \doteq \text{diag}(\tilde{d}_\pi) \in \mathbb{R}^{|\mathcal{S}| \times |\mathcal{A}| \times |\mathcal{S}|}$ with $\tilde{d}_\pi(s, a) \doteq d_\pi(s)\pi(a|s)$. Then \bar{T} is a contraction mapping w.r.t. some weighted maximum norm, and \bar{v}_π is its unique fixed point. We have $\bar{v}_\pi = D_\pi^{-1}(I - P_\pi^\top \Gamma)^{-1} \tilde{P}_\pi^\top \tilde{D}_\pi r$.

The proof of Theorem 1 is based on Sutton et al. (2016); Zhang et al. (2019, 2020c) and is detailed in the appendix. Theorem 1 states that the numerical value of $\bar{v}_\pi(\text{L1})$ approximately answers Question 2. When Question 2 is asked for a large enough t , the error in the answer $\bar{v}_\pi(\text{L1})$ is arbitrarily small. We call $\bar{v}_\pi(s)$ a *Reverse General Value Function*, which approximately encodes the retrospective knowledge, i.e., the answer to the retrospective question induced by π, r, γ, t and s .

Based on the reverse Bellman operator \bar{T} , we now present the Reverse TD algorithm. Let us consider linear function approximation with a feature function $x : \mathcal{S} \rightarrow \mathbb{R}^K$, which maps a state to a K -dimensional feature. We use $X \in \mathbb{R}^{|\mathcal{S}| \times K}$ to denote the feature matrix, each row of which is $x(s)^\top$. Our estimate for \bar{v}_π is then Xw , where $w \in \mathbb{R}^K$ contains the learnable parameters. At time step t , Reverse TD computes w_{t+1} as

$$w_{t+1} \doteq w_t + \alpha_t (R_t + \gamma(S_{t-1})x_{t-1}^\top w_t - x_t^\top w_t)x_t, \quad (1)$$

where $x_t \doteq x(S_t)$ is shorthand, and $\{\alpha_t\}$ is a deterministic positive nonincreasing sequence satisfying the Robbins-Monro condition (Robbins and Monro, 1951), i.e., $\sum_t \alpha_t = \infty, \sum_t \alpha_t^2 < \infty$. We have

Proposition 1. *(Convergence of Reverse TD) Under Assumption 1, assuming X has linearly independent columns, then the iterate $\{w_t\}$ generated by Reverse TD (Eq (1)) satisfies $\lim_{t \rightarrow \infty} w_t = -\bar{A}^{-1}\bar{b}$ with probability 1, where $\bar{A} \doteq X^\top (P_\pi^\top \Gamma - I) D_\pi X$, $\bar{b} \doteq X^\top \tilde{P}_\pi^\top \tilde{D}_\pi r$.*

The proof of Proposition 1 is based on the proof of the convergence of linear TD in Bertsekas and Tsitsiklis (1996). In particular, we need to show that \bar{A} is negative definite. Details are provided in the appendix. For a sanity check, it is easy to verify that in the tabular setting (i.e., $X = I$), $-\bar{A}^{-1}\bar{b} = \bar{v}_\pi$ indeed holds. Inspired by the success of TD(λ) (Sutton, 1988) and COP-TD(λ) (Hallak and Mannor, 2017), we also extend Reverse TD to Reverse TD(λ), which updates w_{t+1} as

$$w_{t+1} \doteq w_t + \alpha_t \left(R_t + \gamma(S_{t-1})((1 - \lambda)x_{t-1}^\top w_t + \lambda \bar{G}_{t-1}) - x_t^\top w_t \right) x_t.$$

With $\lambda = 1$, Reverse TD(λ) reduces to supervised learning.

Distributional Learning. In anomaly detection with Reverse GVFs, we compare the observed quantity (a scalar) with our retrospective knowledge (a scalar, the conditional expectation). It is not clear how to translate the difference between the two scalars into a decision about whether there is an anomaly. If our retrospective knowledge is a distribution instead, we can perform anomaly detection from a probabilistic perspective. To this end, we propose Distributional Reverse TD, akin to Bellemare et al. (2017); Rowland et al. (2018).

We use $\eta_t^s \in \mathcal{P}(\mathbb{R})$ to denote the conditional probability distribution of \bar{G}_t given $S_t = s$, where $\mathcal{P}(\mathbb{R})$ is the set of all probability measures over the measurable space $(\mathbb{R}, \mathcal{B}(\mathbb{R}))$, with $\mathcal{B}(\mathbb{R})$ being the Borel sets of \mathbb{R} . Moreover, we use $\eta_t \in (\mathcal{P}(\mathbb{R}))^{|\mathcal{S}|}$ to denote the vector whose s -th element is η_t^s . By the definition of \bar{G}_t , we have for any $E \in \mathcal{B}(\mathbb{R})$

$$\eta_t^s(E) = \int_{\mathbb{R} \times \mathcal{S}} (f_{r,\bar{s}} \# \eta_{t-1}^{\bar{s}})(E) d\Pr(S_{t-1} = \bar{s}, R_t = r | S_t = s), \quad (2)$$

where $f_{r,\bar{s}} : \mathbb{R} \rightarrow \mathbb{R}$ is defined as $f_{r,\bar{s}}(x) = r + \gamma(\bar{s})x$, and $f_{r,\bar{s}}\#\eta_{t-1}^{\bar{s}} : \mathcal{B}(\mathbb{R}) \rightarrow [0, 1]$ is the push-forward measure, i.e., $(f_{r,\bar{s}}\#\eta_{t-1}^{\bar{s}})(E) \doteq \eta_{t-1}^{\bar{s}}(f_{r,\bar{s}}^{-1}(E))$, where $f_{r,\bar{s}}^{-1}(E)$ is the preimage of E . To study η_t^s when $t \rightarrow \infty$, we define

$$p(\bar{s}, r|s) \doteq \lim_{t \rightarrow \infty} \Pr(S_{t-1} = \bar{s}, R_t = r | S_t = s) = \frac{d_\pi(\bar{s})}{d_\pi(s)} \sum_{\bar{a}} \pi(\bar{a}|\bar{s}) p(s|\bar{s}, \bar{a}) \Pr(r|\bar{s}, \bar{a}).$$

When $t \rightarrow \infty$, Eq (2) suggests $\eta_t^s(E)$ evolves according to $\eta_t^s(E) = \int_{\mathbb{R} \times \mathcal{S}} (f_{r,\bar{s}}\#\eta_{t-1}^{\bar{s}})(E) d p(\bar{s}, r|s)$. We, therefore, define the distributional reverse Bellman operator $\tilde{\mathcal{T}} : (\mathcal{P}(\mathbb{R}))^{|\mathcal{S}|} \rightarrow (\mathcal{P}(\mathbb{R}))^{|\mathcal{S}|}$ as $(\tilde{\mathcal{T}}\eta)^s \doteq \int_{\mathbb{R} \times \mathcal{S}} (f_{r,\bar{s}}\#\eta^{\bar{s}}) d p(\bar{s}, r|s)$. We have

Proposition 2. *Under Assumption 1, $\tilde{\mathcal{T}}$ is a contraction mapping w.r.t. a metric d , and we refer to its fixed point as η_π . Assuming $\mu_0 = d_\pi$, then $\lim_{t \rightarrow \infty} d(\eta_t, \eta_\pi) = 0$.*

We now provide a practical algorithm to approximate η_π^s based on quantile regression, akin to Dabney et al. (2017). We use N quantiles with quantile levels $\{\tau_i\}_{i=1,\dots,N}$, where $\tau_i \doteq \frac{(i-1)/N + i/N}{2}$. The measure η_π^s is approximated with $\frac{1}{N} \sum_{i=1}^N \delta_{q_i(s;\theta)}$, where δ_x is a Dirac at x , $q_i(s;\theta)$ is a quantile corresponding to the quantile level τ_i , and θ is learnable parameters. Given a transition (s, a, r, s') , we train θ to minimize the following quantile regression loss

$$L(\theta) \doteq \sum_{i=1}^N \sum_{j=1}^N \rho_{\tau_i}^\kappa \left(r + \frac{\gamma(s)}{N} \sum_{k=1}^N q_j(s; \bar{\theta}) - \frac{1}{N} \sum_{k=1}^N q_i(s'; \bar{\theta}) \right),$$

where $\bar{\theta}$ contains the parameters of the target network (Mnih et al., 2015), which is synchronized with θ periodically, and $\rho_{\tau_i}^\kappa(x) \doteq |\tau_i - \mathbb{I}_{x < 0}| \mathcal{H}_\kappa(x)$ is the quantile regression loss function. $\mathcal{H}_\kappa(x)$ is the Huber loss, i.e., $\mathcal{H}_\kappa(x) \doteq 0.5x^2 \mathbb{I}_{x \leq \kappa} + \kappa(|x| - 0.5\kappa) \mathbb{I}_{x > \kappa}$, where κ is a hyperparameter. Dabney et al. (2017) provide more details about quantile-regression-based distributional RL.

Off-policy Learning. We would also like to be able to answer to Question 2 without making the microdrone do a random walk, i.e., we may have another policy μ for the microdrone to collect data. In this scenario, we want to learn \bar{v}_π off-policy. We consider Off-policy Reverse TD, which updates w_t as:

$$w_{t+1} \doteq w_t + \alpha_t \tau(S_{t-1}) \rho(S_{t-1}, A_{t-1}) (R_t + \gamma(S_{t-1}) x_{t-1}^\top w_t - x_t^\top w_t) x_t, \quad (3)$$

where $\tau(s) \doteq \frac{d_\pi(s)}{d_\mu(s)}$, $\rho(s, a) \doteq \frac{\pi(a|s)}{\mu(a|s)}$ and $\{S_0, A_0, R_1, S_1, \dots\}$ is obtained by following the behavior policy μ . Here we assume access to the density ratio $\tau(s)$, which can be learned via Hallak and Mannor (2017); Gelada and Bellemare (2019); Nachum et al. (2019); Zhang et al. (2020a,b).

Proposition 3. *(Convergence of Off-policy Reverse TD) Under Assumption 1, assuming X has linearly independent columns, and the chain induced by μ is ergodic, then the iterate $\{w_t\}$ generated by Off-policy Reverse TD (Eq (3)) satisfies $\lim_{t \rightarrow \infty} w_t = -\bar{A}^{-1} \bar{b}$ with probability 1.*

Off-policy Reversed TD converges to the same point as on-policy Reverse TD. This convergence relies heavily on having the true density ratio $\tau(s)$. When using a learned estimate for the density ratio, approximation error is inevitable and thus convergence is not ensured. It is straightforward to consider a GTD (Sutton et al., 2009b,a; Maei, 2011) analogue, Reverse GTD, as Zhang et al. (2020c) does in Gradient Emphasis Learning. The convergence of Off-Policy Reverse GTD is straightforward (Zhang et al., 2020c), but to a different point from On-policy Reverse TD.

4 Experiments

The Effect of λ . At time step t , the reverse return \bar{G}_t is known and can approximately serve as a sample for $\bar{v}_\pi(S_t)$. It is natural to model this as a regression task where the input is S_t , and the target is \bar{G}_t . This is indeed Reverse TD(1). So we first study the effect of λ in Reverse TD(λ). We consider the microdrone example in Figure 1. The dynamics are specified in Section 1. The reward function and the discount function are specified in Section 2. The policy π is uniformly random. We use a tabular representation and compute the ground truth \bar{v}_π analytically. We vary λ in $\{0, 0.3, 0.7, 0.9, 1.0\}$. For each λ , we use a constant step size α tuned from $\{10^{-3}, 5 \times 10^{-3}, 10^{-2}, 5 \times 10^{-2}\}$. We report the Mean Value Error (MVE) against training steps in Figure 2. At a time step t , assuming our estimation is \bar{V} , the MVE is computed as $\|\bar{V} - \bar{v}_\pi\|_2^2$. The results show that the bias of the estimate decreases quickly at the beginning. As a result, variance of the update target becomes the major obstacle in the learning process, which explains why the best performance is achieved by smaller λ in this experiment.

Anomaly Detection.

Tabular Representation. Consider the microdrone example once again (Figure 1). Suppose we want the microdrone to follow a policy π where $\pi(a_1|s) = 0.1 \forall s$. However, something can go wrong when the microdrone is following π . For example, it may start to take a_1 with probability 0.9 at all states due to a malfunctioning navigation system, which we refer to as a *policy anomaly*. The microdrone may also consume 2% extra battery per step with probability 0.5 due to a malfunctioning engine, which we refer to as a *reward anomaly*, i.e., the reward R_t becomes $R_t + 2$ with probability 0.5. We cannot afford to monitor the microdrone every time step but can do so occasionally, and we hope if something has gone wrong we can discover it. Since it is a microdrone, it does not have the memory to store all the logs between examinations. We now demonstrate that Reverse GVs can discover such anomalies using only constant memory and computation.

Our experiment consists of two phases. In the first phase, we train Reverse GVs off-policy. Our behavior policy μ is uniformly random with $\mu(a_1|s) = 0.5 \forall s$. The target policy is π with $\pi(a_1|s) = 0.1 \forall s$. Given a transition (s, a, r, s') following μ , we update the parameters θ , which is a look-up table in this experiment, to minimize $\rho(s, a)L(\theta)$. In this way, we approximate η_π^s with $N = 20$ quantiles for all s . The MVE against training steps is reported in Figure 3a.

In the second phase, we use the learned η_π^s from the first phase for anomaly detection when we actually deploy π . Namely, we let the microdrone follow π for 2×10^4 steps and compute \bar{G}_t on the fly. In the first 10^4 steps, there is no anomaly. In the second 10^4 steps, the aforementioned *reward anomaly* or *policy anomaly* happens every step. We aim to discover the anomaly via computing the likelihood that \bar{G}_t is sampled from $\eta_\pi^{S_t}$, namely, we compute

$$\text{prob}_{\text{anomaly}}(\bar{G}_t) \doteq 1 - \eta_\pi^{S_t}([\bar{G}_t - \Delta, \bar{G}_t + \Delta]),$$

where Δ is a hyperparameter and we use $\Delta = 1$ in our experiments. We do not have access to $\eta_\pi^{S_t}$ but only N estimated quantiles $\{q_i(S_t; \theta)\}_{i=1, \dots, N}$. To compute $\text{prob}_{\text{anomaly}}(\bar{G}_t)$, we need to first find a distribution whose quantiles are $q_i(S_t; \theta)$. This operation is referred to as imputation in Rowland et al. (2018). Such a distribution is not unique. The commonly used imputation strategy for quantile-regression-based distributional RL is $\frac{1}{N} \sum_{i=1}^N \delta_{q_i(S_t; \theta)}$ (Dabney et al., 2017). This distribution, however, makes it difficult to compute $\text{prob}_{\text{anomaly}}(\bar{G}_t)$. Inspired by the fact that a Dirac can be regarded as the limit of a normal distribution with decreasing scale, we define our approximation for $\eta_\pi^{S_t}$ as $\hat{\eta}_\pi^{S_t} \doteq \frac{1}{N} \sum_{i=1}^N \mathcal{N}(q_i(S_t; \theta), \sigma^2)$, where σ is a hyperparameter and we use $\sigma = 1$ in our experiments. Note $\hat{\eta}_\pi^{S_t}$ does not necessarily have the quantiles $q_i(S_t; \theta)$. We report $1 - \hat{\eta}_\pi^{S_t}([\bar{G}_t - \Delta, \bar{G}_t + \Delta])$ against time steps in Figure 3b. When the anomaly occurs after the first 10^4 steps, the probability of anomaly reported by Reverse GVF becomes high.

Non-linear Function approximation. We now consider Reacher from OpenAI gym (Brockman et al., 2016) and use neural networks as a function approximator for $q_i(s; \theta)$. Our setup is the same as the tabular setting except that the tasks are different. For a state s , we define $\gamma(s) = 0$ if the distance between the end of the robot arm and the target is less than 0.02. Otherwise we always have $\gamma(s) = 1$. When the robot arm reaches a state s with $\gamma(s) = 0$, the arm and the target are reinitialized randomly. We first train a deterministic policy μ_d with TD3 (Fujimoto et al., 2018) achieving an average episodic return of -4 . In the first phase, we use a Gaussian behavior policy $\mu(s) \doteq \mathcal{N}(\mu_d(s), 0.5^2)$. The target policy is $\pi(s) \doteq \mathcal{N}(\mu_d(s), 0.1^2)$. In the second phase, we consider two kinds of anomaly. In the *policy anomaly*, we consider three settings where the policy $\pi(s)$ becomes $\mathcal{N}(\mu_d(s), 0.9^2)$, $\mathcal{N}(\mu_d(s), 1.8^2)$, and $\mathcal{N}(\mu_d(s), 2.7^2)$ respectively. In the *reward anomaly*, we consider three settings where with probability 0.5 the reward R_t becomes $R_t - 1$, $R_t - 5$, and $R_t - 10$ respectively. We report the estimated probability of anomaly in Figure 3c. When an anomaly happens after the first 10^4 steps, the probability of anomaly reported by Reverse GVF becomes high.

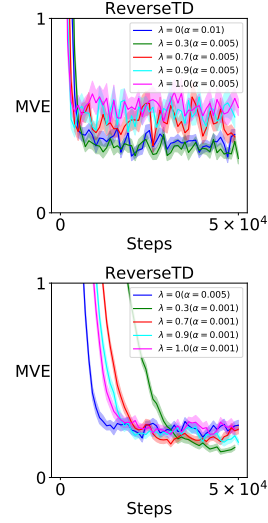


Figure 2: Left: the step size α is tuned to minimize the area under the curve, a proxy for learning speed. Right: the step size α is tuned to minimize the MVE at the end of training. All curves are averaged over 30 independent runs with shaded regions indicate standard errors.

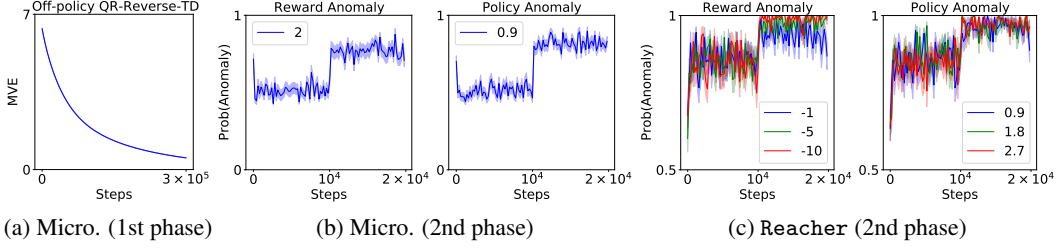


Figure 3: All curves are averaged over 30 independent runs with shaded regions indicate standard errors. (a) MVE against training steps in the first phase of the microdrone example. (b) Anomaly probability in the second phase of the microdrone example. (c) Anomaly probability in the second phase of Reacher, with three different reward anomalies and policy anomalies.

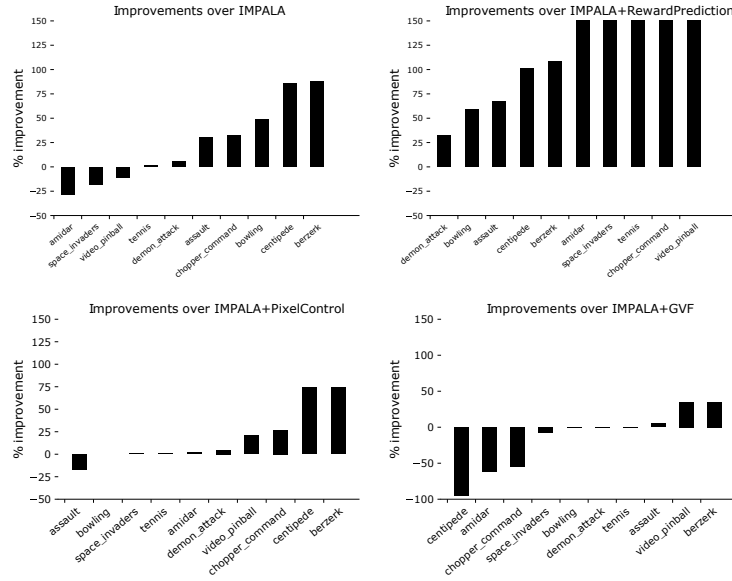


Figure 4: The performance improvement of IMPALA+ReverseGVF over plain IMPALA, IMPALA+RewardPrediction, IMPALA+PixelControl, and IMPALA+GVF. All agents are trained for 2×10^8 steps, the performance is the evaluation performance at the end of training, and the results are averaged over 3 seeds.

Representation Learning. Veeriah et al. (2019) show that automatically discovered GVFs can be used as auxiliary tasks (Jaderberg et al., 2016) to improve representation learning, yielding a performance boost in the main task. Let r and γ be the reward function and the discount factor of the main task. Veeriah et al. (2019) propose two networks for solving the main task: a main task and answer network, parameterized by θ , and a question network, parameterized by ϕ . The two networks do not share parameters. The question network takes as input states and outputs two scalars, representing a reward signal \hat{r} and a discount factor $\hat{\gamma}$. The θ -network has two heads with a shared backbone. The backbone represents the internal state representation of the agent. One head represents the policy π , as well as the value function $v_{\pi, r, \gamma}$, for the main task. The other head represents the answer to the *predictive question* specified by $\pi, \hat{r}, \hat{\gamma}$, i.e., this head represents the value function $v_{\pi, \hat{r}, \hat{\gamma}}$. At time step t , θ is updated to minimize two losses $L_{RL}(\theta_t)$ and $L_{GVF}(\theta_t)$. Here $L_{RL}(\theta_t)$ is the usual RL loss for π and $v_{\pi, r, \gamma}$, e.g., Veeriah et al. (2019) consider the loss used in IMPALA (Espeholt et al., 2018). $L_{GVF}(\theta_t)$ is the TD loss for training $v_{\pi, \hat{r}, \hat{\gamma}}$ with \hat{r} and $\hat{\gamma}$. Minimizing $L_{RL}(\theta_t)$ improves the policy π directly, and Veeriah et al. (2019) show that minimizing $L_{GVF}(\theta_t)$, the loss of the auxiliary task, facilitates the learning of π by improving representation learning. Every K steps,

the question network is updated to minimize $L_{\text{meta}}(\phi) \doteq \sum_{i=t-K}^t L_{\text{RL}}(\theta_i)$. In this way, the question network is trained to propose useful predictive questions for learning the main task.

We now show that automatically discovered Reverse GVFs can also be used as auxiliary tasks to improve the learning of the main task. We propose an IMPALA+ReverseGVF agent, which is the same as the IMPALA+GVF agent in Veeriah et al. (2019) except that we replace $L_{\text{GVF}}(\theta_t)$ with $L_{\text{ReverseGVF}}(\theta_t)$. Here $L_{\text{ReverseGVF}}(\theta_t)$ is the Reverse TD loss for training the reverse general value function $\bar{v}_{\pi, \hat{r}, \hat{\gamma}}$ with \hat{r} and $\hat{\gamma}$, and the $\bar{v}_{\pi, \hat{r}, \hat{\gamma}}$ -head replaces the $v_{\pi, \hat{r}, \hat{\gamma}}$ -head in Veeriah et al. (2019). We benchmark our IMPALA+ReverseGVF agent against a plain IMPALA agent, an IMPALA+RewardPrediction agent, an IMPALA+PixelControl agent, and an IMPALA+GVF agent in ten Atari games. The IMPALA+RewardPrediction agent predicts the immediate reward of the main task of its current state-action pair as an auxiliary task (Jaderberg et al., 2016). The IMPALA+PixelControl agent maximizes the change in pixel intensity of different regions of the input image as an auxiliary task (Jaderberg et al., 2016). According to Veeriah et al. (2019), those ten Atari games are the ten where the IMPALA+PixelControl agent achieves the largest improvement over the plain IMPALA agent over all 57 Atari games.

The results in Figure 4 show that IMPALA+ReverseGVF yields a performance boost over plain IMPALA in 7 out of 10 tested games, and the improvement is larger than 25% in 5 games. IMPALA+ReverseGVF outperforms IMPALA+RewardPrediction in all 10 tested games, indicating reward prediction is not a good auxiliary task for an IMPALA agent in those ten games. IMPALA+ReverseGVF outperforms IMPALA+PixelControl in 8 out of 10 tested games, though the games are selected in favor of IMPALA+PixelControl. IMPALA+ReverseGVF also outperforms IMPALA+GVF, the state-of-the-art in discovering auxiliary tasks, in 3 games. Overall, our empirical study confirms that ReverseGVFs are useful inductive bias for composing auxiliary tasks, though not achieving a new state of the art. We conjecture that IMPALA+GVF outperforms IMPALA+ReverseGVF because GVF aligns better with the main task than ReverseGVF in that the value function of the main task itself is also a GVF.

5 Related Work

Our reverse return \bar{G}_t is inspired by the followon trace F_t in Sutton et al. (2016), which is defined as $F_t \doteq i(S_t) + \gamma(S_t)\rho_{t-1}F_{t-1}$, where $i : \mathcal{S} \rightarrow [0, \infty)$ is a user-defined interest function specifying user’s preference for different states. Sutton et al. (2016) use the followon trace to reweight value function update in Emphatic TD. Later on, Zhang et al. (2020c) propose to learn the conditional expectation $\lim_{t \rightarrow \infty} \mathbb{E}[F_t | S_t = s]$ with function approximation in off-policy actor-critic algorithms. This followon trace perspective is one origin of bootstrapping in the reverse direction, and the followon trace is used only for stabilizing off-policy learning. The second origin is related to learning the stationary distribution of a policy, which dates back to Wang et al. (2007, 2008) in dual dynamic programming for stable policy evaluation and policy improvement. Later on, Hallak and Mannor (2017); Gelada and Bellemare (2019) propose stochastic approximation algorithms (discounted) COP-TD to learn the density ratio, i.e. the ratio between the stationary distribution of the target policy and that of the behavior policy, to stabilize off-policy learning. Our Reverse TD differs from the discounted COP-TD in that (1) Reverse TD is on-policy and does not have importance sampling ratios, while discounted COP-TD is designed only for off-policy setting, as there is no density ratio in the on-policy setting. (2) Reverse TD uses R_t in the update, while discounted COP-TD uses a carefully designed constant. The third origin is an application of RL in web page ranking (Yao and Schuurmans, 2013), where a different Reverse Bellman Equation is proposed to learn the authority score function. Although the idea of reverse bootstrapping is not new, we want to highlight that this paper is the first to apply this idea for representing retrospective knowledge and show its utility in anomaly detection and representation learning. We are also the first to use distributional learning in reverse bootstrapping, providing a probabilistic perspective for anomaly detection.

Another approach for representing retrospective knowledge is to work directly with a reversed chain like Morimura et al. (2010). First, assume the initial distribution μ_0 is the same as the stationary distribution d_π . We can then compute the posterior action distribution given the next state and the posterior state distribution given the action and the next state using Bayes’ rule: $\Pr(a|s') = \frac{\sum_s d_\pi(s)\pi(a|s)p(s'|s,a)}{d_\pi(s')}$, $\Pr(s|s', a) = \frac{d_\pi(s)\pi(a|s)p(s'|s,a)}{d_\pi(s')}$. We can then define a new MDP with the same state space \mathcal{S} and the same action space \mathcal{A} . But the new policy is the posterior distribution

$\Pr(a|s')$ and the new transition kernel is the posterior distribution $\Pr(s|s', a)$. Intuitively, this new MDP flows in the reverse direction of the original MDP. Samples from the original MDP can also be interpreted as samples from the new MDP. Assuming we have a trajectory $\{S_0, A_0, S_1, A_1, \dots, S_k\}$ from the original MDP following π , we can interpret the trajectory $\{S_k, A_{k-1}, \dots, A_0, S_0\}$ as a trajectory from the new MDP, allowing us to work on the new MDP directly. For example, applying TD in the new MDP is equivalent to applying the Reverse TD in the original MDP. However, in the new MDP, we no longer have access to the policy, i.e., we cannot compute $\Pr(a|s')$ explicitly as it requires both d_π and p , to which we do not have access. This is acceptable in the on-policy setting but renders the off-policy setting infeasible, as we do not know the target policy at all. We, therefore, argue that working on the reversed chain directly is only compatible with on-policy learning.

6 Conclusion

In this paper, we present Reverse GVF for representing retrospective knowledge and formalize the Reverse RL framework. We demonstrate the utility of Reverse GVF in both anomaly detection and representation learning. Investigating Reverse-GVF-based anomaly detection with real world data is a possible future work. In this paper, we investigate Reverse RL in only a policy evaluation sense. Reverse RL for control is also a possible future work.

Broader Impact

Reverse-RL makes it possible to implement anomaly detection with little extra memory. This is particularly important for embedded systems with limited memory, e.g., satellites, spacecrafts, microdrones, and IoT devices. The saved memory can be used to improve other functionalities of those systems. Systems where memory is not a bottleneck, e.g., self-driving cars, benefit from Reverse-RL-based anomaly detection as well, as saving memory saves energy, making them more environment-friendly.

Reverse-RL provides a probabilistic perspective for anomaly detection. So misjudgment is possible. Users may have to make a decision considering other available information as well to reach a certain confidence level. Like any other neural network application, combining neural network with Reverse-RL-based anomaly detection is also vulnerable to adversarial attacks. This means the users, e.g., companies or governments, should take extra care for such attacks when making a decision on whether there is an anomaly or not. Otherwise, they may suffer from property losses. Although Reverse-RL itself does not have any bias or unfairness, if the simulator used to train reverse GVFs is biased or unfair, the learned GVFs are likely to inherit those bias or unfairness. Although Reverse-RL itself does not raise any privacy issue, to make a better simulator for training, users may be tempted to exploit personal data. Like any artificial intelligence system, Reverse-RL-based anomaly detection has the potential to greatly improve human productivity. However, it may also reduce the need for human workers, resulting in job losses.

Acknowledgments and Disclosure of Funding

SZ is generously funded by the Engineering and Physical Sciences Research Council (EPSRC). This project has received funding from the European Research Council under the European Union’s Horizon 2020 research and innovation programme (grant agreement number 637713). The experiments were made possible by a generous equipment grant from NVIDIA.

References

- Bellemare, M. G., Dabney, W., and Munos, R. (2017). A distributional perspective on reinforcement learning. *arXiv preprint arXiv:1707.06887*.
- Bertsekas, D. P. and Tsitsiklis, J. N. (1989). *Parallel and distributed computation: numerical methods*. Prentice hall Englewood Cliffs, NJ.
- Bertsekas, D. P. and Tsitsiklis, J. N. (1996). *Neuro-Dynamic Programming*. Athena Scientific Belmont, MA.

- Borkar, V. S. (2009). *Stochastic approximation: a dynamical systems viewpoint*. Springer.
- Brockman, G., Cheung, V., Pettersson, L., Schneider, J., Schulman, J., Tang, J., and Zaremba, W. (2016). Openai gym. *arXiv preprint arXiv:1606.01540*.
- Dabney, W., Rowland, M., Bellemare, M. G., and Munos, R. (2017). Distributional reinforcement learning with quantile regression. *arXiv preprint arXiv:1710.10044*.
- Espeholt, L., Soyer, H., Munos, R., Simonyan, K., Mnih, V., Ward, T., Doron, Y., Firoiu, V., Harley, T., Dunning, I., et al. (2018). Impala: Scalable distributed deep-rl with importance weighted actor-learner architectures. *arXiv preprint arXiv:1802.01561*.
- Fujimoto, S., van Hoof, H., and Meger, D. (2018). Addressing function approximation error in actor-critic methods. *arXiv preprint arXiv:1802.09477*.
- Gelada, C. and Bellemare, M. G. (2019). Off-policy deep reinforcement learning by bootstrapping the covariate shift. In *Proceedings of the 33rd AAAI Conference on Artificial Intelligence*.
- Hallak, A. and Mannor, S. (2017). Consistent on-line off-policy evaluation. In *Proceedings of the 34th International Conference on Machine Learning*.
- Horn, R. A. and Johnson, C. R. (2012). *Matrix analysis (2nd Edition)*. Cambridge university press.
- Jaderberg, M., Mnih, V., Czarnecki, W. M., Schaul, T., Leibo, J. Z., Silver, D., and Kavukcuoglu, K. (2016). Reinforcement learning with unsupervised auxiliary tasks. *arXiv preprint arXiv:1611.05397*.
- Kingma, D. P. and Ba, J. (2014). Adam: A method for stochastic optimization. *arXiv preprint arXiv:1412.6980*.
- Levin, D. A. and Peres, Y. (2017). *Markov chains and mixing times*. American Mathematical Soc.
- Maei, H. R. (2011). *Gradient temporal-difference learning algorithms*. PhD thesis, University of Alberta.
- Mnih, V., Kavukcuoglu, K., Silver, D., Rusu, A. A., Veness, J., Bellemare, M. G., Graves, A., Riedmiller, M., Fidjeland, A. K., Ostrovski, G., et al. (2015). Human-level control through deep reinforcement learning. *Nature*.
- Morimura, T., Uchibe, E., Yoshimoto, J., Peters, J., and Doya, K. (2010). Derivatives of logarithmic stationary distributions for policy gradient reinforcement learning. *Neural computation*.
- Nachum, O., Chow, Y., Dai, B., and Li, L. (2019). Dualdice: Behavior-agnostic estimation of discounted stationary distribution corrections. *arXiv preprint arXiv:1906.04733*.
- Nair, V. and Hinton, G. E. (2010). Rectified linear units improve restricted boltzmann machines. In *Proceedings of the 27th International Conference on Machine Learning*.
- Puterman, M. L. (2014). *Markov decision processes: discrete stochastic dynamic programming*. John Wiley & Sons.
- Robbins, H. and Monroe, S. (1951). A stochastic approximation method. *The Annals of Mathematical Statistics*.
- Rowland, M., Bellemare, M. G., Dabney, W., Munos, R., and Teh, Y. W. (2018). An analysis of categorical distributional reinforcement learning. *arXiv preprint arXiv:1802.08163*.
- Sutton, R. S. (1988). Learning to predict by the methods of temporal differences. *Machine Learning*.
- Sutton, R. S. (2009). The grand challenge of predictive empirical abstract knowledge. In *Working Notes of the IJCAI-09 Workshop on Grand Challenges for Reasoning from Experiences*.
- Sutton, R. S. and Barto, A. G. (2018). *Reinforcement Learning: An Introduction (2nd Edition)*. MIT press.

- Sutton, R. S., Maei, H. R., Precup, D., Bhatnagar, S., Silver, D., Szepesvári, C., and Wiewiora, E. (2009a). Fast gradient-descent methods for temporal-difference learning with linear function approximation. In *Proceedings of the 26th International Conference on Machine Learning*.
- Sutton, R. S., Maei, H. R., and Szepesvári, C. (2009b). A convergent $o(n)$ temporal-difference algorithm for off-policy learning with linear function approximation. In *Advances in Neural Information Processing Systems*.
- Sutton, R. S., Mahmood, A. R., and White, M. (2016). An emphatic approach to the problem of off-policy temporal-difference learning. *The Journal of Machine Learning Research*.
- Sutton, R. S., Modayil, J., Delp, M., Degris, T., Pilarski, P. M., White, A., and Precup, D. (2011). Horde: A scalable real-time architecture for learning knowledge from unsupervised sensorimotor interaction. In *Proceedings of the 10th International Conference on Autonomous Agents and Multiagent Systems*.
- Veeriah, V., Hessel, M., Xu, Z., Rajendran, J., Lewis, R. L., Oh, J., van Hasselt, H. P., Silver, D., and Singh, S. (2019). Discovery of useful questions as auxiliary tasks. In *Advances in Neural Information Processing Systems*.
- Wang, T., Bowling, M., and Schuurmans, D. (2007). Dual representations for dynamic programming and reinforcement learning. In *2007 IEEE International Symposium on Approximate Dynamic Programming and Reinforcement Learning*.
- Wang, T., Bowling, M., Schuurmans, D., and Lizotte, D. J. (2008). Stable dual dynamic programming. In *Advances in neural information processing systems*.
- White, M. (2017). Unifying task specification in reinforcement learning. In *Proceedings of the 34th International Conference on Machine Learning*.
- Yao, H. and Schuurmans, D. (2013). Reinforcement ranking. *arXiv preprint arXiv:1303.5988*.
- Yu, H. (2015). On convergence of emphatic temporal-difference learning. In *Conference on Learning Theory*.
- Yu, H., Mahmood, A. R., and Sutton, R. S. (2018). On generalized bellman equations and temporal-difference learning. *The Journal of Machine Learning Research*.
- Zhang, R., Dai, B., Li, L., and Schuurmans, D. (2020a). Gendice: Generalized offline estimation of stationary values. In *International Conference on Learning Representations*.
- Zhang, S., Boehmer, W., and Whiteson, S. (2019). Generalized off-policy actor-critic. In *Advances in Neural Information Processing Systems*.
- Zhang, S., Liu, B., and Whiteson, S. (2020b). Gradientdice: Rethinking generalized offline estimation of stationary values. In *Proceedings of the 37th International Conference on Machine Learning*.
- Zhang, S., Liu, B., Yao, H., and Whiteson, S. (2020c). Provably convergent two-timescale off-policy actor-critic with function approximation. In *Proceedings of the 37th International Conference on Machine Learning*.

A Failure in Representing Retrospective Knowledge with GVFs

One may consider answering Question 2 with GVF via setting L4 to be the initial state and terminating an episode when the microdrone gets to L1. Then the value of L4 seems to be the answer to Question 2. To understand how this approach fails, let us consider transitions L4 \rightarrow L3 \rightarrow L4 \rightarrow L1. It then becomes clear that we are unable to design a Markovian reward for the transition L3 \rightarrow L4. This reward has to be non-Markovian to cancel all previously accumulated rewards. To make the reward Markovian, one may augment the state space with the battery level, which significantly increases the size of the state space. More importantly, this renders off-policy learning infeasible. The transition kernel on this augmented state space depends on the original reward function. So we cannot use off-policy learning to learn a GVF associated with a different reward function, as changing the reward function changes the transition kernel on the augmented state space. We can, of course, include the information about the new reward function into the augmented space. This, however, indicates the size of the state space grows exponentially with the number of reward functions we want to consider in off-policy learning. There is even a deeper defect. Let us consider the setting where we have two charging stations, say L2 and L4. Then if we want to use GVF directly as aforementioned assuming the aforementioned issues could somehow be solved, we need to set the initial state to L2 and L4 respectively. We then solve the two MDPs and compute $v(L2)$ and $v(L4)$ respectively. Finally, we may need to compute $d_\pi(L2)v(L2) + d_\pi(L4)v(L4)$ as the answer, where d_π is the stationary distribution of the original MDP, which is, unfortunately, unknown. To summarize, there may be some retrospective knowledge that GVF can represent if enough tweaks are applied. But in general, representing retrospective with GVF suffers from poor generality and poor scalability.

B Proofs

Lemma 1. (Corollary 6.1 in page 150 of Bertsekas and Tsitsiklis (1989)) *If Y is a square nonnegative matrix and $\rho(Y) < 1$, then there exists some vector $w \succ 0$ such that $\|Y\|_\infty^w < 1$. Here \succ is elementwise greater and $\rho(\cdot)$ is the spectral radius. For a vector y , its w -weighted maximum norm is $\|y\|_\infty^w \doteq \max_i |y_i| w_i$. For a matrix Y , $\|Y\|_\infty^w \doteq \max_{y \neq 0} \frac{\|Yy\|_\infty^w}{\|y\|_\infty^w}$.*

B.1 Proof of Theorem 1

Proof. Given the similarity between \bar{G}_t and the followon trace F_t as discussed in Section 5, the existence of $\lim_{t \rightarrow \infty} \mathbb{E}_{\pi,p,r}[\bar{G}_t | S_t = s]$ can be established in exactly the same way as Zhang et al. (2019) establish the existence of $\lim_{t \rightarrow \infty} [F_t | S_t = s]$ in their Lemma 1. We therefore omit this to avoid verbatim repetition. We have

$$\begin{aligned}
 \bar{v}_\pi(s) &\doteq \lim_{t \rightarrow \infty} \mathbb{E}[\bar{G}_t | S_t = s] \\
 &= \lim_{t \rightarrow \infty} \mathbb{E}[R_t + \gamma(S_{t-1})\bar{G}_{t-1} | S_t = s] \\
 &= \lim_{t \rightarrow \infty} \sum_{\bar{s}, \bar{a}} \Pr(S_{t-1} = \bar{s}, A_{t-1} = \bar{a} | S_t = s) \mathbb{E}[R_t + \gamma(S_{t-1})\bar{G}_{t-1} | S_{t-1} = \bar{s}, A_{t-1} = \bar{a}] \\
 &\hspace{15em} \text{(Law of total expectation)} \\
 &= \sum_{\bar{s}, \bar{a}} \frac{d_\pi(\bar{s})\pi(\bar{a}|\bar{s})p(s|\bar{s}, \bar{a})}{d_\pi(s)} \left(r(\bar{s}, \bar{a}) + \gamma(\bar{s})\bar{v}_\pi(\bar{s}) \right) \quad \text{(Bayes' rule)} \tag{4}
 \end{aligned}$$

The matrix form of Eq (4) is exactly $\bar{v}_\pi = D_\pi^{-1} \tilde{P}_\pi^\top \tilde{D}_\pi r + D_\pi^{-1} P_\pi^\top \Gamma D_\pi \bar{v}_\pi$, solving which leads to $\bar{v}_\pi = D_\pi^{-1} (I - P_\pi^\top \Gamma)^{-1} \tilde{P}_\pi^\top \tilde{D}_\pi r$. Assumption 1 implies $\rho(P_\pi^\top \Gamma) < 1$. As $Y_1 Y_2$ and $Y_2 Y_1$ have the same eigenvalues (e.g., see Theorem 1.3.22 in Horn and Johnson (2012)), we have $\rho(D_\pi^{-1} P_\pi^\top \Gamma D_\pi) = \rho(P_\pi^\top \Gamma D_\pi D_\pi^{-1}) < 1$. Lemma 1 then implies \bar{T} is a contraction mapping w.r.t. some weighted maximum norm. \square

B.2 Proof of Proposition 1

We first state a lemma about the convergence of the following iterates

$$w_{t+1} = w_t + \alpha_t (A(Y_t)w_t + b(Y_t)),$$

where $\{Y_t\}$ is a Markov chain evolving in \mathcal{Y} , $w_t \in \mathbb{R}^K$, $A : \mathcal{Y} \rightarrow \mathbb{R}^{K \times K}$, $b : \mathcal{Y} \rightarrow \mathbb{R}^K$.

Assumption 2. (Assumption 4.5 in Bertsekas and Tsitsiklis (1996))

(a) The step sizes α_t are nonnegative, deterministic, and satisfy $\sum_t \alpha_t = \infty$, $\sum_t \alpha_t^2 < \infty$.

(b) The chain $\{Y_t\}$ has a stationary distribution p_Y .

(c) The matrix $\bar{A} \doteq \mathbb{E}_{y \sim p_Y}[A(y)]$ is negative definite.

(d) There is a constant C_0 such that $\|A(y)\| \leq C_0$ and $\|b(y)\| \leq C_0$.

(e) There exists scalars $0 < C_1, 0 < \rho < 1$ such that

$$\|\mathbb{E}[A(Y_t)] - \bar{A}\| \leq C_1 \rho^t, \quad \|\mathbb{E}[b(Y_t)] - \bar{b}\| \leq C_1 \rho^t,$$

where $\bar{b} \doteq \mathbb{E}_{y \sim p_Y}[b(y)]$.

Lemma 2. (Proposition 4.8 in Bertsekas and Tsitsiklis (1996))

Under Assumption 2, $\lim_{t \rightarrow \infty} w_t = -\bar{A}^{-1}\bar{b}$ with probability 1.

We now prove Theorem 1 via verifying Assumption 2 thus invoking Lemma 2.

Proof. We first consider a deterministic reward setting, i.e., we assume $R_{t+1} = r(S_t, A_t)$. The Reverse TD update Eq (1) can be rearranged as

$$w_{t+1} = w_t + \alpha_t(A(Y_t)w_t + b(Y_t)),$$

where $Y_t \doteq (X_{t-1}, A_{t-1}, X_t)$, $y = (s, a, s')$, $A(y) \doteq \gamma(s)x(s')x(s)^\top - x(s')x(s')^\top$, $b(y) \doteq r(s, a)x(s')$. It is easy to verify that $\bar{A} \doteq \mathbb{E}_{y \sim p_Y}[A(y)] = X^\top(P_\pi^\top \Gamma - I)D_\pi X$ and $\bar{b} \doteq \mathbb{E}_{y \sim p_Y}[b(y)] = \tilde{P}_\pi^\top \tilde{D}_\pi r$. Assumption 2(a) is satisfied automatically. Obviously $\{Y_t\}$ is ergodic and its stationary distribution is $p_Y(y) \doteq d_\pi(s)\pi(a|s)p(s'|s, a)$. Assumption 2(b) is now satisfied.

We now verify Assumption 2(c). Our proof is inspired by the proof of Lemma 6.4 in Bertsekas and Tsitsiklis (1996). Let $z \in \mathbb{R}^{|S|}/\{0\}$, we aim to show $z^\top \bar{A} z < 0$. As X has linearly independent columns, it suffices to show $z^\top D_\pi(\Gamma P_\pi - I)z < 0$. We have

$$\begin{aligned} \|\Gamma P_\pi z\|_{D_\pi}^2 &= \sum_s d_\pi(s) \gamma(s)^2 \left(\sum_{s'} P_\pi(s, s') z(s') \right)^2 \leq \sum_{s, s'} d_\pi(s) \gamma(s)^2 P_\pi(s, s') z(s')^2 \\ &\leq \sum_{s, s'} d_\pi(s) P_\pi(s, s') z(s')^2 = \sum_{s'} d_\pi(s') z(s')^2 = \|z\|_{D_\pi}^2, \end{aligned}$$

where the first inequality comes from Jensen's inequality, whose equality holds iff all components of z are the same scalar (referred to as $z_c \neq 0$). When that happens, we have $\|\Gamma P_\pi z\|_{D_\pi}^2 = z_c^2 \sum_s d_\pi(s) \gamma(s)^2$. Note there exists at least one s such that $\gamma(s) < 1$, otherwise $(\Gamma P_\pi - I)$ is singular, violating Assumption 1. So $\|\Gamma P_\pi z\|_{D_\pi}^2 < z_c^2 = \|z\|_{D_\pi}^2$. To conclude, for any z , we always have $\|\Gamma P_\pi z\|_{D_\pi} < \|z\|_{D_\pi}$, yielding

$$z^\top D_\pi \Gamma P_\pi z \leq \|z\|_{D_\pi}^{\frac{1}{2}} \|\Gamma P_\pi z\|_{D_\pi}^{\frac{1}{2}} = \|z\|_{D_\pi} \|\Gamma P_\pi z\|_{D_\pi} < \|z\|_{D_\pi}^2 = z^\top D_\pi z,$$

which completes the proof.

Assumption 2(d) is straightforward as \mathcal{Y} is finite. Assumption 2(e) is trivial in our setting as we do not have eligibility trace and can be obtained from standard arguments about the mixing time of MDP (e.g., Theorem 4.9 in Levin and Peres (2017)).

The extension from deterministic rewards to stochastic rewards is standard (e.g., see Section 2.2 in Borkar (2009)) thus omitted. \square

B.3 Proof of Proposition 2

Proof. Assumption 1 implies $\rho(P_\pi^\top \Gamma) < 1$. Then Lemma 1 implies that there exists a w in $\mathbb{R}^{|S|}$ such that $k_0 \doteq \|P_\pi^\top \Gamma\|_\infty^w < 1$. Let ℓ_2 be the Cramér distance in $\mathcal{P}(\mathbb{R})$ (see Definition 3 in Rowland et al.

(2018)), for any $\eta_1, \eta_2 \in (\mathcal{P}(\mathbb{R}))^{|\mathcal{S}|}$, we have

$$\begin{aligned}
\ell_2^2\left((\bar{\mathcal{T}}\eta_1)^s, (\bar{\mathcal{T}}\eta_2)^s\right) &= \ell_2^2\left(\int_{\mathbb{R} \times \mathcal{S}} (f_{r,\bar{s}} \# \eta_1^{\bar{s}}) d p(\bar{s}, r|s), \int_{\mathbb{R} \times \mathcal{S}} (f_{r,\bar{s}} \# \eta_2^{\bar{s}}) d p(\bar{s}, r|s)\right) \\
&\leq \int_{\mathbb{R} \times \mathcal{S}} \ell_2^2\left(f_{r,\bar{s}} \# \eta_1^{\bar{s}}, f_{r,\bar{s}} \# \eta_2^{\bar{s}}\right) d p(\bar{s}, r|s) \\
&= \int_{\mathbb{R} \times \mathcal{S}} \gamma(\bar{s}) \ell_2^2\left(\eta_1^{\bar{s}}, \eta_2^{\bar{s}}\right) d p(\bar{s}, r|s) \\
&= \sum_{\bar{s}} p(\bar{s}|s) \gamma(\bar{s}) \ell_2^2\left(\eta_1^{\bar{s}}, \eta_2^{\bar{s}}\right),
\end{aligned} \tag{5}$$

where the inequality comes from Jensen's inequality and the next equality comes from a property of ℓ_2 . We refer the reader to the proof of Proposition 2 in Rowland et al. (2018) for details. Let ℓ_2^{2,η_1,η_2} be a vector in $\mathbb{R}^{|\mathcal{S}|}$ with the s -th element $\ell_2^{2,\eta_1,\eta_2}(s) \doteq \ell_2^2(\eta_1^s, \eta_2^s)$, the RHS of Eq (5) is then $(P_\pi^\top \Gamma \ell_2^{2,\eta_1,\eta_2})(s)$. We have

$$\begin{aligned}
\max_s \ell_2^2\left((\bar{\mathcal{T}}\eta_1)^s, (\bar{\mathcal{T}}\eta_2)^s\right) / w_s &\leq \max_s (P_\pi^\top \Gamma \ell_2^{2,\eta_1,\eta_2})(s) / w_s = \|P_\pi^\top \Gamma \ell_2^{2,\eta_1,\eta_2}\|_\infty^w \\
&\leq k_0 \|\ell_2^{2,\eta_1,\eta_2}\|_\infty^w = k_0 \max_s \ell_2^2\left(\eta_1^{\bar{s}}, \eta_2^{\bar{s}}\right) / w_s,
\end{aligned}$$

indicating

$$\max_s \ell_2\left((\bar{\mathcal{T}}\eta_1)^s, (\bar{\mathcal{T}}\eta_2)^s\right) / \sqrt{w_s} \leq \sqrt{k_0} \max_s \ell_2\left(\eta_1^{\bar{s}}, \eta_2^{\bar{s}}\right) / \sqrt{w_s}. \tag{6}$$

With $d(\eta_1, \eta_2) \doteq \max_s \ell_2\left(\eta_1^s, \eta_2^s\right) / \sqrt{w_s}$, we have

$$\begin{aligned}
d(\eta_1, \eta_2) + d(\eta_2, \eta_3) &= \max_s \ell_2(\eta_1^s, \eta_2^s) / \sqrt{w_s} + \max_s \ell_2(\eta_2^s, \eta_3^s) / \sqrt{w_s} \\
&\geq \max_s \left(\ell_2(\eta_1^s, \eta_2^s) + \ell_2(\eta_2^s, \eta_3^s) \right) / \sqrt{w_s} \\
&\geq \max_s \ell_2(\eta_1^s, \eta_3^s) / \sqrt{w_s} = d(\eta_1, \eta_3).
\end{aligned}$$

In other words, d satisfies the triangle inequality, indicating d is indeed a valid metric. Eq (6) then implies that $\bar{\mathcal{T}}$ is a $\sqrt{k_0}$ -contraction in d . Standard fixed point theories then imply that $\bar{\mathcal{T}}$ has a unique fixed point, which we refer to as η_π .

As $\mu_0 = d_\pi$, we have $p(\bar{s}, r|s) = \Pr(S_{t-1} = \bar{s}, R_t = r | S_t = s)$ holds for all t . Then Eq (2) implies that $\eta_t = \bar{\mathcal{T}}\eta_{t-1}$, from which $\lim_{t \rightarrow \infty} d(\eta_t, \eta_\pi) = 0$ follows directly. \square

B.4 Proof of Proposition 3

Proof. The proof is the same as the proof of Theorem 1 except that we define

$$\begin{aligned}
A(y) &\doteq \tau(s) \rho(s, a) (\gamma(s) x(s') x(s)^\top - x(s') x(s')^\top), \\
b(y) &\doteq \tau(s) \rho(s, a) r(s, a) x(s').
\end{aligned}$$

As we consider off-policy setting, the stationary distribution of $\{Y_t\}$ is then $p_Y(y) \doteq d_\mu(s) \mu(a|s) p(s'|s, a)$. It is easy to verify that we still have $\bar{A} \doteq \mathbb{E}_{y \sim p_Y}[A(y)] = X^\top (P_\pi^\top \Gamma - I) D_\pi X$ and $\bar{b} \doteq \mathbb{E}_{y \sim p_Y}[b(y)] = \bar{P}_\pi^\top \bar{D}_\pi r$. The rest is thus the same. \square

C Experiment Details

C.1 Anomaly Detection

The TD3 agent used for generating μ_d is the same as Fujimoto et al. (2018), which is trained for 2×10^4 steps in Reacher to achieve an average episodic return of -4. We use two hidden-layer neural networks with ReLU (Nair and Hinton, 2010) activation function. Each hidden layer consists of 64 units. The output layer has 20 units, representing 20 quantiles. We use an Adam (Kingma and Ba, 2014) optimizer with an initial learning rate 5×10^{-3} . The size of the experience replay buffer is 10^4 and the mini-batch size is 128. We update the target network every 100 steps. We conduct our experiments on an Nvidia DGX-1 with PyTorch, though no GPU is used.

C.2 Representation Learning

As our IMPALA+ReverseGVF agent is simply replacing the canonical TD loss in the IMPALA+GVF agent with the Reverse TD loss, we refer the reader to Veeriah et al. (2019) for all the implementation details.